Study on USV Cluster Formation Control and Cooperative Obstacle Avoidance

Yuan Hsiang Chen
National Taiwan University of Science and Technology, Taiwan

Alex Paul
Niger Delta University, Nigeria

Abstract: With the deepening of research on unmanned vehicles, research on USV (Unmanned Surface Vehicle) has gradually become extensive. In order to cope with complex Marine operations, the study of USV cluster collaborative operations has been emphasized. Therefore, this paper explores USV cluster formation and collaborative obstacle avoidance. In this paper, a formation control method of USV cluster is proposed based on the leader-follower architecture and the consistency algorithm. To solve the problem of formation cooperative obstacle avoidance, the traditional APF (APF method) is improved to avoid falling into the local optimal, and the cluster cooperative obstacle avoidance method is proposed. Finally, the simulation results show that the USV cluster formation control and obstacle avoidance methods are effective.

Keywords: USV Cluster Formation, Leader–Follower, Coordinated Obstacle Avoidance, Improved APF Method.

Introduction

In recent years, unmanned vehicle technology has been developing rapidly, and the UAV and unmanned vehicle as the object of extensive research. However, with the continuous expansion of research areas and the continuous development of Marine resources in various countries, the related research of USV, another object of unmanned vehicles, is also paying more and more attention (Arrais et al., 2017). Nowadays, it has also gradually realized such basic functions as mission planning, path planning, trajectory tracking and attitude control (Zhou et al., 2020) for single craft. However, as offshore operations become more complex and the offshore environment becomes more diverse, a single USV cannot meet the needs of operations. In order to improve the efficiency and scope of offshore operations, the research of USV cluster system is becoming the focus. In the control of the USV cluster system, it is

Correspondents Author:
Alex Paul, Department of Electrical Engineering, Niger Delta University, Nigeria
Email : alex.paul66@gmail.com

necessary to consider not only the path planning of each boat, but also the coordinated movement of the whole formation. Especially, when encountering obstacles, it is necessary to restore the formation of the cluster after each USV in the formation completes obstacle avoidance. Therefore, the research on USVs cluster control can be roughly divided into two levels, one is formation control of USVs cluster system, the other is collaborative collision avoidance method of cluster (Choudhary et al., 2022).

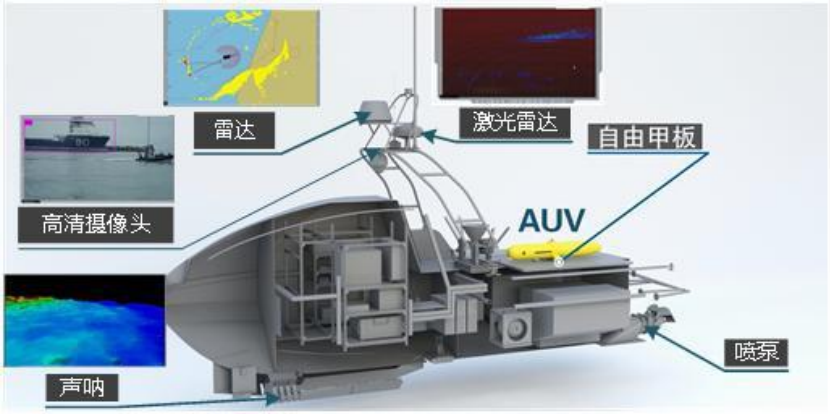

Figure 1 USV Structure Diagram

For formation control of USV cluster system, the current mainstream methods include control based on agent behaviour (Balch & Arkin, 1998), control dependent on virtual structure (Minetto et al., 2017), and the design of leader-follower structure (Do, 2012) to achieve predetermined formation shape control. Among the above design architectures, due to the simplicity and scalability of the leader-follower architecture, it is more suitable for the USVs cluster applied on the sea (Cao et al., 2012). The main feature of this architecture is that the leader can guide the follower to conduct group behaviour in formation along the pre-planned reference route, and the follower can also act as the leader of another USV. In (Cui et al., 2010), an efficient leader-follower formation control algorithm is proposed for a USV cluster, which uses an approximation-based technique to force vehicle formation to move along the target trajectory in a given pattern. In (Peng et al., 2017), a graceful leader-follower formation control scheme based on constrained distance and Angle tracking errors is proposed. Therefore, the leader-follower architecture is more suitable for USV cluster formation operating at sea.

For the collision avoidance problem of USV cluster system, at present, the main solutions of multi-agent obstacle avoidance control problem include grid method, neural network method, swarm intelligence algorithm, APF method, etc. (Jin, 2016). Most of these collision avoidance planning algorithms cannot plan an optimal collision avoidance path for USV in a short time. Due to its complex principle, large amount of computation and long planning time, swarm intelligent algorithm is not suitable for USV cluster collision avoidance on complex sea surface, especially for collision avoidance of local obstacles, it is difficult to meet the real-time

requirements. The APF method has the simple principle, the small amount of computation and the fast calculation speed, which is convenient for the real-time control of the lower level, in the real-time obstacle avoidance and smooth trajectory control, has been widely used. In (Yang et al., 2022), an adaptive APF cost function is added to the event-triggered model predictive control (EMPC) for autonomous electric vehicles, which reduces the amount of computation, improves the robustness, and enables vehicles to effectively avoid obstacles in trajectory tracking. In (Feng et al., 2018), the application of APF method to UAV cluster obstacle avoidance also achieves good obstacle avoidance and trajectory tracking effects. In (Chen et al., 2021), for the path planning problem of USV offshore operations, APF method is introduced to avoid local encounters and effectively avoid unknown obstacles in navigation. However, because the traditional APF method is easy to fall into the local optimal solution and the target may be unreachable, this paper improves the traditional APF method and then applies it to the obstacle avoidance control of USV cluster.

However, for the study of USVs cluster, the main problems are how to keep the formation of USVs unchanged in formation, how to organize the movement of USVs cluster formation, and how to restore the formation after obstacle avoidance if there is a need to avoid obstacles. Based on the above questions, this paper has carried out related exploration and research. In this paper, the leader-follower architecture is used to realize the formation of USVs cluster, and the improved APF method is used for real-time collision avoidance control of the whole cluster. The leader-follower architecture adopted in this paper uses the consistency algorithm to achieve formation control and the APF method to avoid obstacles, which gets a good result in the simulation. The rest of this article is structured as follows. In the second section, the distributed control structure model of the leader-follower formation is established, and the consistency algorithm is used to realize the formation control based on the graph theory. The third section gives the principle of the improved obstacle avoidance method of APF. In Section 4, a series of simulation results are provided to verify and evaluate the proposed algorithm. Section 5 summarizes this paper and looks forward to further research in the future.

Research Method

Leader-Follower Model Building

USVs Cluster System Communication Diagram

Controlling a collaborative USVs cluster dynamic system is a dynamic problem of interconnecting with each other through a communication diagram that illustrates the flow of

information between each node (Geng et al., 2022). The goal of cooperative control is to design a control protocol for each node to ensure the state synchronization behaviour of all nodes in a certain sense. In a collaborative system, any control protocol must carry out distributed control according to its prescribed graph topology, that is to say, the control protocol of each node is only allowed to rely on the information about the node and its neighbour nodes in the graph, and the communication restrictions imposed by the topology may seriously limit the work that the local distributed control protocol on each node can accomplish (Lin et al., 2021).

In the USVs cluster collaborative formation, we are concerned with the behaviour and interaction of dynamic systems that are interconnected through links in a communication network modelled as a graph with directed edges corresponding to the flow of information allowed between the systems. Each USV in the formation is modelled as a node in the graph. The basic question then becomes how the graph topology interacts with the local feedback control protocol of the nodes to generate the overall behaviour of the interconnecting nodes (Luo et al., 2023).

A topology can be expressed as $G = (V, E)$, including $V = v_1, \dots, v_n$ said N a collection collection of nodes, E said E edge set, assuming that the graph is simple directed graph, namely $(v_i, v_j \notin E)$ and the same to no multiple edges between nodes, the elements in the collection of $E(v_i, v_j)$ said from node v_j point node v_i edge, said information in the fleet from node v_j

USV flow node v_i USV, Node v_i out of USV d_i^o said as the number of data sending side edge, in-degree d_i said as the number of data to collect the edge. To sense A weight a_{ij}, which can be an adjacency matrix or connectivity matrix $A = [a_{ij}]$ said, including when $(v_i, v_j \notin E), a_{ij} = 1$, otherwise $a_{ij} = 0$ the weighted into the degree of node i at this time can be expressed as the matrix A line the *ith* the sum of all values, as shown in Equation 1:

$$d_i = \sum_{j=1}^{N} a_{ij} \tag{1}$$

Then the weighted output can be expressed as the Equation 2:

$$d_i^o = \sum_{j=1}^{N} a_{ij} \tag{2}$$

Both the in degree and out degree are local properties of the graph. In formation topology communication, the out degree can reflect the influence of the node on other USV of the formation, that is, the greater the influence of the node USV on the formation consistency.

Define a diagonal into degree matrix $D = diagd_i$ and graph Laplacian $L = D - A$, many properties of the figure can be found from research, the nature of the graph Laplacian in the dynamic multi-node system has extremely important significance in the research of graph theory and a directed graph and its adjoint matrix, diagonal matrix and Laplacian as shown in Figure 2:

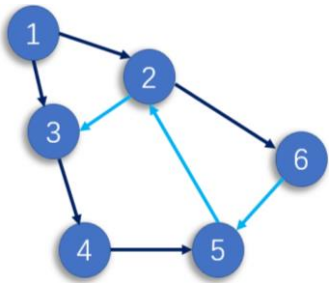

Figure 2 The Directed Graph G

The corresponding matrix is as follows:

$$A = \begin{bmatrix} 0 & 0 & 1 & 0 & 0 & 0 \\ 1 & 0 & 0 & 0 & 0 & 1 \\ 1 & 1 & 0 & 0 & 0 & 0 \\ 0 & 1 & 0 & 0 & 0 & 0 \\ 0 & 0 & 1 & 0 & 0 & 0 \\ 0 & 0 & 0 & 1 & 1 & 0 \end{bmatrix} D = \begin{bmatrix} 1 & 0 & 0 & 0 & 0 & 0 \\ 0 & 2 & 0 & 0 & 0 & 0 \\ 0 & 0 & 2 & 0 & 0 & 0 \\ 0 & 0 & 0 & 1 & 0 & 0 \\ 0 & 0 & 0 & 0 & 1 & 0 \\ 0 & 0 & 0 & 0 & 0 & 2 \end{bmatrix} L = \begin{bmatrix} 1 & 0 & -1 & 0 & 0 & 0 \\ -1 & 2 & 0 & 0 & 0 & -1 \\ -1 & -1 & 2 & 0 & 0 & 0 \\ 0 & -1 & 0 & 1 & 0 & 0 \\ 0 & 0 & -1 & 0 & 1 & 0 \\ 0 & 0 & 0 & -1 & 0 & 2 \end{bmatrix}$$

The characteristic structure of the Laplacian matrix L plays a key role in the dynamic system analysis on the graph. The following is the analysis of the eigenvalue of L, and the reduction form of the Laplacian matrix is defined as follows:

$$L = MJM^{-1} \tag{3}$$

Where, the formal matrix J and the transformation matrix M are:

$$J = \begin{vmatrix} \lambda_1 & 1 & & \\ & \lambda_2 & 1 & \\ & & \cdots & 1 \\ & & & \lambda_N \end{vmatrix}, M = [v_1 \quad v_2 \quad \cdots \quad v_N] \tag{4}$$

Where the eigenvalue λ_i and the right eigenvector v_i of M satisfy:

$$(\lambda_i I - L)v_i = 0 \tag{5}$$

Where is the identity matrix I. The left eigenvector w_i of matrix M satisfies:

$$w_i(\lambda_i I - L) = 0 \tag{6}$$

$$w_i^T v_i = 1 \tag{7}$$

Since the sum of all the row elements of the matrix L is 0, if and only if there is a unique eigenvector C of L whose eigenvalue $Lc = 0$ is 0, that is, when L rank is $N - 1$, graph G has a spanning tree, which plays an important role in the stability of formation.

Leader-Follower Formation Control Algorithm Based on Consistency

In this paper, the distributed control structure of the leader-follower formation is adopted, and the consistency algorithm given below is adopted to realize the formation control based on the diagram theory above. Leader-follower formation is a classical formation form. The main idea of the first-order formation algorithm based on consistency is to control the relative position and speed between the leader and the follower. When these values reach a certain stable state, the formation is realized, in which the lead USV plays a crucial role. The first-order continuous system model of the formation system is as follows:

$$\dot{x}_i = u_i \tag{8}$$

Where, respectively, x_i, u_i represents the state quantity and input quantity of the node, and $x_i, u_i \in R^n, n$ represents the dimension of the state quantity. In an ideal case, the following form of control input is considered:

$$u = \sum_{j \in N_i} a_{ij}(x_j - x_i) \tag{9}$$

Where a_{ij} is the formation adjacency matrix element and N_i is the neighbor set of members i. By substituting Equation 9 into Equation 8 and introducing the global state variable $x = [x_1 \cdots x_n]^T \in R^n$, the global dynamic relationship can be obtained as follows:

$$\dot{x} = -Dx + Ax = -Lx \tag{10}$$

From the above equation, we can see that the closed-loop dynamic characteristics of formation depend on the matrix L. In addition, if and only if the topology G of the formation has a spanning tree, the eigenvalues of $-L$ are all located in the left half plane of the complex plane, so Equation 9 can ensure the consistency of the system, and the final state value is:

$$c = \sum_{i=1}^{N} p_i x_i(0) \tag{11}$$

Under discrete time, Equation 8 can be reduced to:

$$x_i(k+1) = x_i(k) + u_i(k) \tag{12}$$

In this paper, a scenario is assumed that the leader leads other USVs to complete a distance movement and move from the starting point to a target point. Ideally, the algorithm of the follower in the formation adopts the following form:

$$u_N(k) = m + kD(k) + \sum_{i \in N_i} a_{N_i} r_{N_i}(k) \tag{13}$$

Where, r_{N_i} denotes the relative position between the pilot and other USVs, m and k are all constants, and $D(k)$ denotes the distance between the pilot and the target point at time k. The speed of the pilot is affected by the adjacent nodes and the distance between the pilot and the target point.

Obstacle Avoidance Algorithm of APF Method

The basic idea of the APF method is to construct the repulsive potential field around the obstacle and the gravitational potential field around the target point, which is similar to the electromagnetic field in physics. The controlled object is subjected to the repulsive force and the gravitational force in the compound field composed of these two potential fields. The combined force of the repulsive force and the gravitational force guides the motion of the controlled object and searches the collision free obstacle avoidance path. More intuitively, the potential field method compares the obstacle to the peak with high potential energy value on the plain, while the target point is the trough with low potential energy value, as shown in Figure 3.

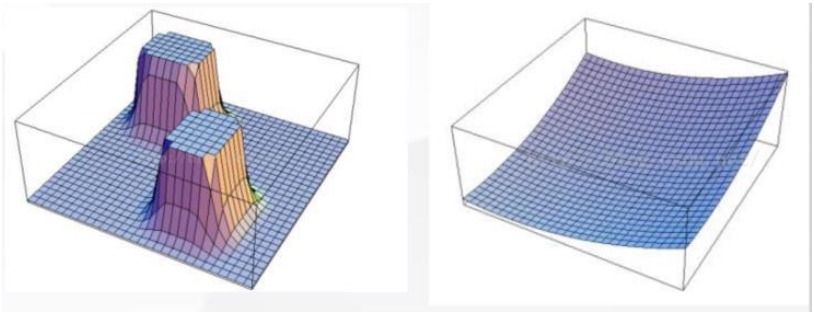

Figure 3 Diagram of Repulsive Force Field (Left) and Gravitational Field (Right)

Principle of APF Method

Gravitational Potential Field

The gravitational potential field is mainly related to the distance between the USV and the target point. The greater the distance, the greater the potential energy value of the USV. The smaller the distance is, the smaller the potential value of USV is, so the function of the gravitational potential field is:

$$U_{att}(q) = \frac{1}{2}\eta\rho^2(q, q_g) \tag{14}$$

Where η is the positive proportional gain coefficient and $\rho^2(q, q_g)$ is a vector representing the Euclidean distance between the USV position q and the target point q_g. The vector $|q, q_g|$ direction is from the USV position to the target point position.

The corresponding gravity $F_{att}(q)$ is the negative gradient of the gravitational field, representing the direction of the fastest change of the gravitational potential field function $U_{att}(q)$, and its relation is as follows:

$$F_{att}(q) = -\nabla U_{att}(q) = -\eta\rho(q, q_g) \tag{15}$$

Repulsive Potential Field

The factor that determines the repulsive potential field of the obstacle is the distance between the USV and the obstacle. When the USV does not enter the influence range of the obstacle, its potential energy value is zero. After the USV enters the sphere of influence of the obstacle, the greater the distance between the two, the smaller the potential energy value of the USV, and the smaller the distance, the greater the potential energy value of the USV. The potential field function of the repulsive force potential field is:

$$U_{req}(q) = \begin{cases} \frac{1}{2}k\left(\frac{1}{\rho(q, q_0)} - \frac{1}{\rho_0}\right)^2, & 0 \le \rho(q, q_0) \le \rho_0 \\ 0, & \rho(q, q_0) > \rho_0 \end{cases} \tag{16}$$

Where k is the direct proportionality coefficient, $\rho(q, q_0)$ is a vector, the direction is from the obstacle to the USV, the magnitude is the Euclidean distance $|q, q_0|$ between the USV and the obstacle, ρ_0 is a constant, represents the maximum influence range of the obstacle's effect on the USV.

According to Equation 16, the repulsive potential field is different from the gravitational potential field, and USV is not always subjected to the repulsive action of obstacles on it. When the relative distance between the USV and the obstacle exceeds ρ_0, it is determined that the obstacle has no effect on the USV. When the USV enters the influence range of the obstacle, that is, when the relative distance between the USV and the obstacle is less than ρ_0, the USV begins to be affected by the repulsive force of the obstacle. The smaller the relative distance between the USV and the obstacle is, the greater the repulsive effect is, and the potential energy increases. The greater the relative distance between the USV and the obstacle, the smaller the repulsive force and the lower its potential energy. The corresponding repulsive force is the negative gradient force of the repulsive potential field:

$$F_{req}(q) = \begin{cases} k\left(\frac{1}{\rho(q,q_0)} - \frac{1}{\rho_0}\right)\frac{1}{\rho^2(q,q_0)}, 0 \le \rho(q,q_0) \le \rho_0 \\ 0, \qquad\qquad \rho(q,q_0) > \rho_0 \end{cases} \tag{17}$$

Net Force Potential Field

According to the gravitational field function and repulsive field function defined above, the composite field of the entire operating space can be obtained. The resultant potential field size of USV is the sum of the repulsive potential field and the gravitational potential field received by USV. Therefore, the total function of the resultant potential field is:

$$U(q) = U_{att}(q) + U_{req}(q) \tag{18}$$

The resultant force is:

$$F(q) = -\nabla U(q) = F_{att}(q) + F_{req}(q) \tag{19}$$

The direction of the resultant force determines the driving direction of USV, and the magnitude of the resultant force determines the driving acceleration of USV.

Improvement of APF Method

Local Optimal Problem of Traditional APF Method

Since the distance between the obstacle and the target point is too close, when the USV reaches the target point, according to the potential field function, the attraction of the target point decreases to zero, while the repulsive force of the obstacle is not zero. At this time, although the USV reaches the target point, it cannot stop under the action of the repulsive force field, thus causing the problem of the unreachable target. In addition, in some special cases, the traditional APF method is easy to fall into the problem of local optimization. The two most typical cases are as follows:

a) As shown in Figure 4., when the Angle between the repulsive force of the obstacle and the gravitational force of the target point is approximately 180°, almost in the same straight line, the problem of the USV falling into local optimal in front of the obstacle will occur.

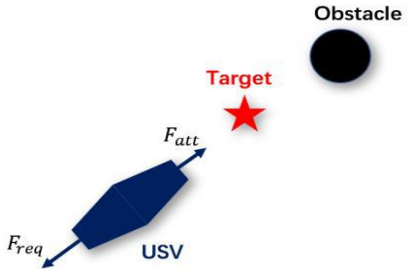

Figure 4 The traditional APF method falls into the local optimal case (1)

b) As shown in Figure 5, if the repulsive force of several obstacles is equal to and opposite to the gravitational force of the target point, then the resultant force is 0. USV itself determines that it reaches the position of minimum potential energy, but does not reach the desired target point. Since the net force is zero, the USV is stuck in a position of minimal potential energy, unable to continue forward and turn to reach the desired target point.

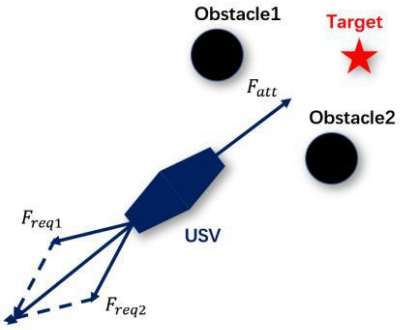

Figure 5 The Traditional APF Method Falls Into The Local Optimal Case（2）

Improved Barrier Repulsion Potential Field Function

The problem of local optimum and target unreachable is solved by improving the repulsive potential field function of obstacles. By adding a regulating factor ρ_g^n to the obstacle repulsion field model of the traditional APF method, only when USV reaches the target point can both the repulsion and the attraction decrease to zero, thus solving the problems of local optimization and target unreachable. The improved repulsive force field function is:

$$U_{req}(q) = \begin{cases} \frac{1}{2}k\left(\frac{1}{\rho(q,q_0)} - \frac{1}{\rho_0}\right)^2 \rho_g^n, 0 \le \rho(q,q_0) \le \rho_0 \\ 0, \qquad\qquad \rho(q,q_0) > \rho_0 \end{cases} \tag{20}$$

ρ_g^n is the distance between USV and the target point, where n is the optional normal number.

$$\begin{cases} F_{req} = F_{req1} + F_{req2} \\ F_{req1} = k\left(\dfrac{1}{\rho(q,q_0)} - \dfrac{1}{\rho_0}\right)\dfrac{\rho_g^n}{\rho^2(q,q_0)} \\ F_{req2} = \dfrac{n}{2}k\left(\dfrac{1}{\rho(q,q_0)} - \dfrac{1}{\rho_0}\right)^2 \rho_g^{n-1} \end{cases} \tag{21}$$

Where, F_{req1} the direction is that the obstacle points to USV, and F_{req2} the direction of, is that USV points to the target point. The distance between USV and the target point is added into the improved repulsive field function, so that the gravitational force and the repulsive force received by USV in the process of driving to the target decrease to a certain extent, and only when USV reaches the target point, the gravitational force and the repulsive force decrease to zero at the same time, that is, the target point becomes the minimum point of potential energy value. Thus, the problems of local optimal and target unreachable can be solved.

Combination of Swarm Formation Control and APF Method for Obstacle Avoidance

In the actual process of movement, USV will use its own sensor (such as Lidar) to scan and detect the surrounding environment, as shown in Figure 6:

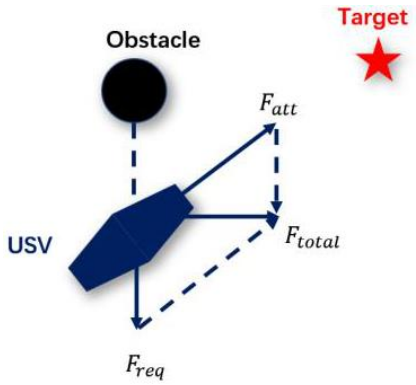

Figure 6 USV Sensor

Assuming that the USV can detect the coordinates X_{obs} of obstacles within a certain range (including other USVs) at time k, the obstacles will have a repulsive F_{req} effect on the speed of the USV J, which satisfies:

$$F_{req\ j}(k) = \sum_{l=1}^{M} \alpha\left(x_j(k) - x_{obs}^l\right) \tag{22}$$

Where, M is the number of obstacles, $\alpha = \frac{\frac{1}{d_j(k)} - \frac{1}{d_M}}{\delta - d}$, $d_j(k) = \left\| X_{F_{req}} - X_j(k) \right\|$, d_M, is the detection distance, and δ is a constant. At this time, the obstacle avoidance response $F_{req}(k)$ will have an impact on the USV speed. Currently, the pilot control model in the formation is as follows:

$$u_N(k) = m + kD(k) + \sum_{i \in N_i} a_{N_I} r_{N_i}(k) + \beta F_{req\ i}(k) \tag{23}$$

Where β is a constant, and the control algorithm of the follower is:

$$u_i(k) = \varepsilon \sum_{j \in N_i} a_{ij} \left(x_j(k) - x_i(k) - r_{ij}(k) \right) + \beta F_{req\ i}(k) \tag{24}$$

This influence enables USVs to effectively avoid obstacles on the basis of maintaining the original formation to the maximum extent and will grow larger as the distance between obstacles becomes closer, thus ensuring the safety of each USV.

Result and Discussion

Establishment of Simulation Model

In order to verify the algorithm and model proposed in this paper, the USV cluster formation simulation model with leader-follower architecture was established based on the MATLAB experimental environment, and the improved APF algorithm was used to simulate the obstacle avoidance.

USV Formation Simulation

Firstly, the USV cluster formation communication structure can be represented by a directed graph $G = (V, E)$, where $V = 1, 2, \ldots, N$ the representation graph has N vertices, then E represents an edge composed of vertices $E \subset V \times V$. In the directed graph, information can only be transmitted from the parent node to the child node. This paper takes 1 leader and 4 followers as an example to conduct simulation. The formation diagram is shown in Figure 7.

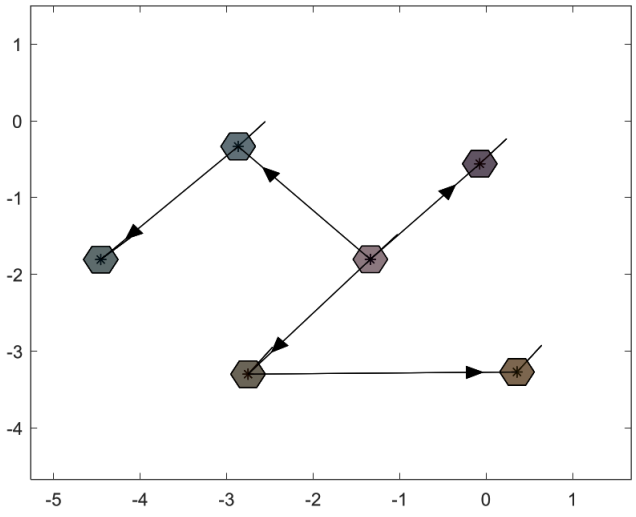

Figure 7 USV Diagram

The adjacency matrix corresponding to the communication topology is shown as follows:

$$A = \begin{bmatrix} 0 & 0 & 0 & 0 & 0 & 1 \\ 0 & 0 & 0 & 0 & 0 & 1 \\ 1 & 0 & 0 & 0 & 0 & 0 \\ 0 & 0 & 0 & 0 & 0 & 1 \\ 0 & 0 & 0 & 1 & 0 & 0 \\ 0 & 0 & 0 & 0 & 0 & 0 \end{bmatrix} \tag{25}$$

After determining the communication topology, it is necessary to set the initial position information (including coordinates x, y and orientation Angle θ) of each USV and the relative position relationship before the cooperative state reaches stability. The initial location information is set to:

```
init_f=[-4 -1.5 0;
    -2 -2.5 pi/4;
    -6 -2.4 -pi/4;
    -2.5 -4 pi/2;
    -1 -4.5 -pi/2;
    -2.5 -3 0];
pose_x=init_f(:,1);
pose_y=init_f(:,2);
pose_th=init_f(:,3);
pose_x(:,2)=init_f(:,1);
pose_y(:,2)=init_f(:,2);
pose_th(:,2)=init_f(:,3);
```

At the same time, the program is given the position information of the target point $goal$, the upper limit of speed $Kinematic$, the control period dt, the position information of the obstacle ob_temp, the detection distance of the USV $detect\_R$ and the maximum distance of the

communication connection *d_max*. When the position error between the USVs is greater than that, the communication connection will be disconnected.

USV Formation Coordination and Obstacle Avoidance Algorithm Application

In this paper, the leader-follower formation structure is adopted, and the cycle control is set for 1000 times, each control interval is 0.1s, that is, the total movement is 100s.As the obstacle avoidance method adopted in this paper is to improve the APF method, the distance between the USV of the pilot and the target point should be calculated in each control, so that the target point can give the USV of the pilot a gravitational force. The greater the distance, the faster the sailing speed. At the same time, when the obstacle enters the detection distance of the USV, the repulsive force of the obstacle to the USV is calculated, so that the USV can avoid collision with the obstacle and continue to move towards the target point. After calculating the motion information of the leader, it is necessary to calculate the motion information of the other five followers. Firstly, the error information of the leader and the follower is calculated according to the principle of the first order formation coordination, and a certain speed is applied to the leader to make it move towards the coordinated position. Part of the code is as follows:

```
%目标点引力
distance=sqrt((goal(1)-pose_x(N,k))^2+(goal(2)-pose_y(N,k))^2);
th=atan2(goal(2)-pose_y(N,k),goal(1)-pose_x(N,k));
if distance>d_max
   distance=d_max;
end
V_x(N,k+1)=KN*distance*cos(th);
 V_y(N,k+1)=KN*distance*sin(th);
out=confine([V_x(N,k) V_y(N,k)],[V_x(N,k+1) V_y(N,k+1)],Kinematic,0.1
);
%障碍物斥力
ob_pose=ob_temp;
repulsion=compute_repulsion([pose_x(N,k),pose_y(N,k)],ob_pose,detect_
R);
V_x(N,k+1)=V_x(N,k+1)+beta*repulsion(1);
V_y(N,k+1)=V_y(N,k+1)+beta*repulsion(2);
%%协同运动
for j=1:N       %%One-order Consensus control
if A(i,j)==1
      w_ij=2-exp(-((pose_x(j,k-1)-pose_x(i,k)-(delta_x(j)-
delta_x(i)))^2+(pose_y(j,k-1)-pose_y(i,k)-(delta_y(j)-
delta_y(i)))^2));
      sum_delta_x=sum_delta_x+A(i,j)*w_ij*((pose_x(j,k-1)-
pose_x(i,k))-(delta_x(j)-delta_x(i)));
      sum_delta_y=sum_delta_y+A(i,j)*w_ij*((pose_y(j,k-1)-
pose_y(i,k))-(delta_y(j)-delta_y(i)));
       sum_edge_weight=sum_edge_weight+w_ij;
end
end
```

Analysis of Simulation Experiment Results

After the simulation model is established and the program is executed, the following simulation experiment results can be obtained, as shown in Figure.8:

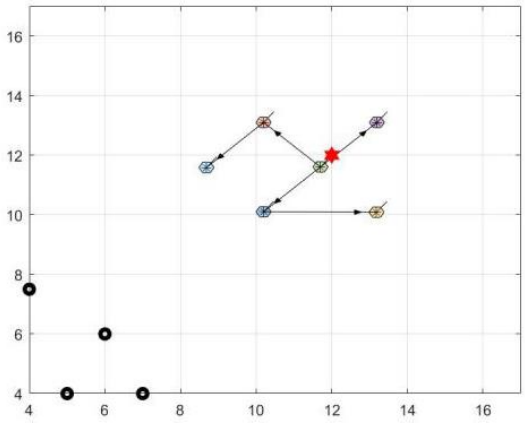

Figure 8 USV Cluster Formation Arrival Terminal Diagram

Figure 8 shows the USV cluster formation, bypassing the obstacles and maintaining maximum formation shape to reach the target point. The black circle represents the obstacle point and the red five-pointed star represents the target point.

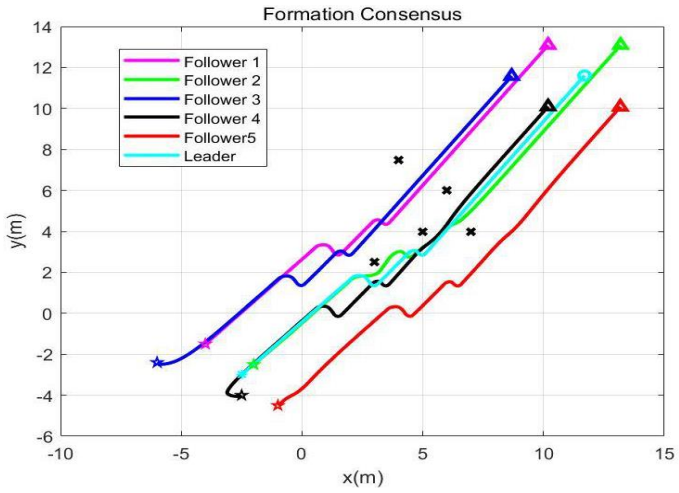

Figure 9 USV Cluster Formation Track Operating Diagram

Figure 9 shows the formation assembly of USV clusters, and the improved APF method can be used to avoid obstacles on the waterway, and finally restore the formation shape. The trajectory diagram of reaching the target point more intuitively demonstrates the effectiveness of the design method in this paper and realizes the obstacle avoidance control of USV cluster formation.

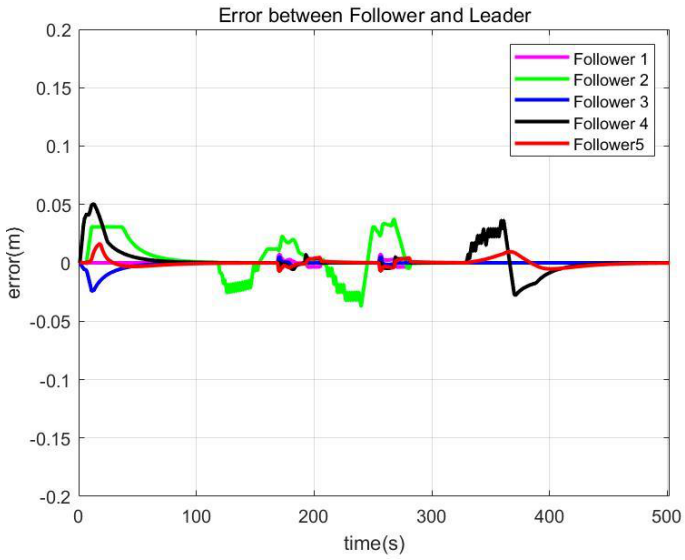

Figure 10 Follower and Leader Relative Position Error

To better verify the effectiveness of the design method in this paper, Figure 10 shows the relative position error between the follower and the leader. It can be intuitively seen from the figure that the relative position error between the two is $\pm 0.05\, m$. When the USV cluster formation is not in the obstacle avoidance state, the relative position error tends to $0\, m$, The effectiveness of USV cluster formation and cooperative obstacle avoidance is further verified.

Conclusions

In this paper, the USV cluster formation control is realized by using the leader-follower architecture and the consistent first-order formation algorithm to control the relative position and speed between the leader and the follower. On the other hand, by improving the traditional APF method, this paper avoids falling into the local optimal in some special cases, solves the problem of target unreachable, and finally realizes the collaborative obstacle avoidance of USV cluster. Through the method designed in this paper, USV cluster formation and cooperative obstacle avoidance can be realized, which has enlightening significance for the control of multi-USV and even multi-robot cluster. In order to further study, the USV cluster control, the real satellite map can be used to carry out the task assignment and obstacle setting in the real environment, and the method designed in this paper can be further verified and improved to make it more practical. In addition, the design of this paper is only a preliminary study and simulation, both formation algorithm and obstacle avoidance algorithm, it has a lot of shortcomings and limitations, in the future research, we can try a variety of methods combination and fusion, to achieve better USV cluster control.

References

Balch, T., & Arkin, R. C. (1998). Behavior-based formation control for multirobot teams. *IEEE Transactions on Robotics and Automation*, *14*(6), 926–939.

Cao, Y., Yu, W., Ren, W., & Chen, G. (2012). An overview of recent progress in the study of distributed multi-agent coordination. *IEEE Transactions on Industrial Informatics*, *9*(1), 427–438.

Chen, Y., Bai, G., Zhan, Y., Hu, X., & Liu, J. (2021). Path planning and obstacle avoiding of the USV based on improved ACO-APF hybrid algorithm with adaptive early-warning. *IEEE Access*, *9*, 40728–40742.

Cui, R., Ge, S. S., How, B. V. E., & Choo, Y. S. (2010). Leader--follower formation control of underactuated autonomous underwater vehicles. *Ocean Engineering*, *37*(17–18), 1491–1502.

Do, K. D. (2012). Formation control of multiple elliptical agents with limited sensing ranges. *Automatica*, *48*(7), 1330–1338.

Feng, Y., Wu, Y., Cao, H., & Sun, J. (2018). Uav formation and obstacle avoidance based on improved apf. *2018 10th International Conference on Modelling, Identification and Control (ICMIC)*, 1–6.

Jin, X. (2016). Fault tolerant finite-time leader--follower formation control for autonomous surface vessels with LOS range and angle constraints. *Automatica*, *68*, 228–236.

Minetto, R., Volpato, N., Stolfi, J., Gregori, R. M. M. H., & Da Silva, M. V. G. (2017). An optimal algorithm for 3D triangle mesh slicing. *Computer-Aided Design*, *92*, 1–10.

Peng, Z., Wang, J., & Wang, D. (2017). Distributed containment maneuvering of multiple marine vessels via neurodynamics-based output feedback. *IEEE Transactions on Industrial Electronics*, *64*(5), 3831–3839.

Yang, H., Wang, Z., Xia, Y., & Zuo, Z. (2022). EMPC with adaptive APF of obstacle avoidance and trajectory tracking for autonomous electric vehicles. *ISA Transactions*.

Zhou, C., Gu, S., Wen, Y., Du, Z., Xiao, C., Huang, L., & Zhu, M. (2020). The review unmanned surface vehicle path planning: Based on multi-modality constraint. *Ocean Engineering*, *200*, 107043. https://doi.org/https://doi.org/10.1016/j.oceaneng.2020.107043

Arrais, R., Oliveira, M., Toscano, C., & Veiga, G. (2017). A mobile robot based sensing approach for assessing spatial inconsistencies of a logistic system. Journal of Manufacturing Systems, 43, 129-138. https://doi.org/https://doi.org/10.1016/j.jmsy.2017.02.016

Choudhary, P. K., Routray, S., Upadhyay, P., & Pani, A. K. (2022). Adoption of enterprise mobile systems – An alternative theoretical perspective. International Journal of Information Management, 67, 102539.

https://doi.org/https://doi.org/10.1016/j.ijinfomgt.2022.102539

Geng, Y., Yuan, M., Tang, H., Wang, Y., Wei, Z., Lin, B., & Zhuang, W. (2022). Robot-based mobile sensing system for high-resolution indoor temperature monitoring. Automation in Construction, 142, 104477. https://doi.org/https://doi.org/10.1016/j.autcon.2022.104477

Lin, T. Y., Shi, G., Yang, C., Zhang, Y., Wang, J., Jia, Z., Guo, L., Xiao, Y., Wei, Z., & Lan, S. (2021). Efficient container virtualization-based digital twin simulation of smart industrial systems. Journal of Cleaner Production, 281, 124443. https://doi.org/https://doi.org/10.1016/j.jclepro.2020.124443

Luo, X., Mu, D., Wang, Z., Ning, P., & Hua, C. (2023). Adaptive full-state constrained tracking control for mobile robotic system with unknown dead-zone input. Neurocomputing, 524, 31-42. https://doi.org/https://doi.org/10.1016/j.neucom.2022.12.025